Lotus-leaf inspired surfaces: hydrophobicity evolution of replicas due to mechanical cleaning and mould wear

Jean-Michel Romano (1)*, Antonio Garcia-Giron (1), Pavel Penchev (1), Mert Gulcur (2), Ben R. Whiteside (2), Stefan Dimov (1)

(1) Department of Mechanical Engineering, School of Engineering, University of Birmingham, B15 2TT Birmingham, United Kingdom

(2) Centre for Polymer Micro & Nano Technology, Faculty of Engineering and Informatics, School of Engineering, University of Bradford, BD7 1DJ Bradford, United Kingdom

* Contact: jean-michel.romano@gadz.org

Abstract

Inspired from the low wetting properties of Lotus leaves, the fabrication of dual micro/nano-scale topographies is of interest to many applications. In this research, superhydrophobic surfaces are fabricated by a process chain combining ultrashort pulsed laser texturing of steel inserts and injection moulding to produce textured polypropylene parts. This manufacturing route is very promising and could be economically viable for mass production of polymeric parts with superhydrophobic properties. However, surface damages, such as wear and abrasion phenomena, can be detrimental to the attractive wetting properties of replicated textured surfaces. Therefore, the final product lifespan is investigated by employing mechanical cleaning of textured polypropylene surfaces with multipurpose cloths following the ASTM D3450 standard. Secondly, the surface damage of replication masters after 350 injection moulding cycles with glass-fiber reinforced polypropylene, especially to intensify mould wear, was investigated. In both cases, the degradation of the dual-scale surface textures had a clear impact on surface topography of the replicas and thus on their wetting properties, too.

Keywords: Wear, abrasion, microtexture, wettability, micro injection moulding, laser texturing.

1. Introduction

Polypropylene (PP) is a common material that finds application in areas such as home appliances, automobile air ducting parts, pipes and many others [1,2], where the injection moulding of thermoplastic parts with tailored wetting properties of their surfaces is of increasing interest. Water repellence observed in nature, e.g. on Lotus leaves or Rose petals, has been inspiring many researchers and several attempts at mimicking their surface structures have been reported [3,4]. In this research, a manufacturing route is considered, employing:

i) ultrashort laser texturing, which is a very attractive technology for fabricating surface structures on metals [4,5] and

ii) injection moulding - a well-established process for replicating surface topographies from textured masters onto polymer parts [6,7].

Similar manufacturing routes employing injection moulding [8] or other techniques [9-13] to replicate laser-textured surfaces have already been reported, especially to produce replicas with engineered hydrophobic surfaces. However, any damage to the surface topography would inevitably impact their wetting response, either due to damage on the final surface [8,14,15] or damage on the mould resulting in indirect damage to the final part.

Therefore, to assess the durability of the textured surfaces used in the investigated process chain, reciprocating abrasive cycles, mimicking real-life cleaning routines, were conducted on textured PP parts. Furthermore, a more abrasive PP compound was used in the injection moulding trials to intensify mould wear and thus to investigate the indirect effects on textured PP replicas. Especially, the evolutions of surface topography and its wetting properties were studied.

2. Materials and methods

2.1 Laser texturing

A stainless steel bar (Uddeholm Stavax ESR, modified AISI 420) was machined to produce inserts with dimensions ∅10 mm x 7 mm. The surfaces of the inserts were polished (S_a = 40 nm) and textured by employing an ultrashort laser (Amplitude Systemes Satsuma, 310 fs pulses, 1032 nm wavelength).

A spot diameter of 30 µm was steered into the focal plane using a 3D scan head (RhoThor RTA) and a telecentric 100 mm focusing lens (see Fig. 1). A Lotus-inspired hierarchical topography with peaks and valleys was fabricated using processing parameters obtained in another study [8] (see Table 1). In particular, a grid-like scanning strategy was employed as depicted in Fig. 1 that included intersecting scan lines under 90° with 25 µm spacing between them. In addition, the scan lines were repeated 50 times employing 7.9 µJ pulses with a pulse-to-pulse distance of 2 µm and thus to produce the intended multi-scale texturing effect, i.e. a peaks-and-valleys micro-structure covered with a laser-induced roughness. After laser-texturing, the inserts were ultrasonically cleaned in ethanol bath for 15 min, rinsed with water and finally dried with compressed air.

Table 1. Laser processing parameters.

Parameters	Units	Values
Pulse energy	µJ	7.9
Pulse repetition rate	kHz	250
Scanning speed	mm/s	500
Spot diameter at focus	µm	30
Pulse-to-pulse distance (d)	µm	2
Hatch distance (h)	µm	25
Number of scans	-	50

2.2 Micro injection moulding

A polypropylene (PP) compound (Ineos PP 100-GA12) was used to produce polymeric parts and investigate the effects of reciprocating cleaning cycles on their textured surfaces. A 30% glass fibre (GF) reinforced PP compound (Borealis Fibremod GD301FE black 9502) was then used in the injection moulding trial to intensify the wear of the textured steel inserts, and thus investigate the impact of mould wear on resulting wetting properties of the replicas.

The textured insert was integrated into a modular mould to produce thermoplastic parts with dimensions ∅17 mm and 0.5 mm using a micromoulding machine (Wittmann Battenfeld MicroPower 15) (see Fig. 2). The micromoulding parameters (see Table 2) were selected based on the material datasheet and a previous study [8], and no demoulding agent was utilised.

Table 2. Micro-injection moulding parameters.

Parameters	Units	Values
Screw temperature profile	°C	200,200,215
Nozzle temperature	°C	230
Mould temperature	°C	60
Injection speed	mm/s	200
Injection pressure	bar	400
Holding pressure	bar	450
Holding time	s	5
Full cycle time	s	25

2.3 Reciprocating cleaning cycles

Usually, harsh mechanical abrasions are performed by various means to judge about the degradation of wetting properties [16–18], but there is not a standardized test to validate the durability of such functional response. In this research, the cleaning cycles were performed in reciprocating mode (see Fig. 3) in a washability tester (Elcometer 1720) by adapting the ASTM D3450 standard that was originally developed for abrasion tests of coatings [19] (see Table 3). The counterpart used in the tester, was a multipurpose cloth (Ubesol) made of fibres of ~13 µm in diameter that had the following composition: 60% viscose, 25% polyester, 15% polypropylene. The cloth was renewed every 125 cycles while the orientation of the textures in regard to the reciprocating movement was randomised. The tests were carried out in dry and wet conditions, with 3:100 of detergent (Fairy original) in distilled water (15 ml poured every 75 cycles). After the tests, any debris or detergent were removed by rinsing the surfaces 3 times with water and drying them with compressed air.

Table 3. Reciprocating cleaning parameters.

Parameters	Units	Values
Full stroke length	mm	180
Load (dry)	kgf/cm^2	0.05
Cycle speed	min^{-1}	37

2.4 Inspection of surface topographies and functionality

The textured PP surfaces were inspected using a focus variation microscope (Alicona G5, IF-MeasureSuite 4.1 software). In particular, the true-to-projected aspect ratio and the peak-to-valley distance (Δz) were measured. The submicron roughness was analysed using a scanning electron microscope (SEM) (Hitachi TEM3030Plus) with a back-scattered secondary electron detector in low vacuum.

The wetting properties of the polymer replica were characterised using an optical tensiometer (Biolin Scientific Attension Theta T2000-Basic+). Employing the sessile drop technique, 6 µl of milliQ water were dispensed in ambient conditions. After stabilisation, the Young-Laplace fitting method was applied to measure the static contact angle (CA).

For the measurement campaign, the average and standard deviation values were calculated from nine measurements.

3. Results and discussion

3.1 Replication of laser-textured surfaces

Figure 4 shows the Lotus-leaf like surface structures that were laser-fabricated on a tool steel insert and then replicated on PP replicas. A laser-induced roughness was covering the micro-scale topography consisting of peaks and valleys with a peak-to-peak distance of 25 µm. Due to the accumulation of energy during the laser processing, single or multiple sporadic holes appeared at the bottom of the valleys. Such sporadic holes could not be measured using a conventional microscopy, due to their apparent high aspect ratio. However, a cross section showed that the holes varied in depth and were covered by a laser-induced roughness.

On the PP replicas, a peak and valley topography with Δz of approximately 32 µm was observed. The surface was covered with laser-induced roughness replicated from the inserts. The peaks of the protrusions were relatively smooth, showing that the high-aspect ratio holes were not fully replicated with the used micromoulding process settings. Further optimisation of the micromoulding process could improve the replication of the laser-textured surfaces.

3.2 Wetting of laser-textured replicas

Figure 5 depicts different wetting states observed in this study. When water (liquid L) gets in contact with PP surfaces, i.e. a solid (S) with a lower surface energy, the contact area between L and S is minimized. Especially, untextured PP surfaces are already in a hydrophobic regime with CA of 105.9°. For a flat surface, Young [20] described the thermodynamic equilibrium of wetting by $\cos\theta_Y = (\gamma_S - \gamma_{SL}) / \gamma_L$, where: θ_Y is the CA; γ_S - the overall surface energy of the surface, γ_L - the overall surface tension of the liquid and γ_{SL} - the interfacial tension between solid/liquid.

Surface textures increased significantly the CA values and they reached 160° on micromoulded PP surfaces. This phenomenon was analytically explained by Wenzel (W) [21]

who introduced a roughness ratio parameter, r_W (≥1), to predict the CA on rough surfaces, θ_W: $\cos\theta_W = r_W \cos\theta_Y$. The W model shows that the surface roughness increases hydrophobicity ($\theta_W > \theta_Y$) of hydrophobic materials ($\theta_Y > 90°$).

In addition, the micromoulded PP surfaces reached a so-called superhydrophobic regime (CA > 150° and low rolling-off angles), leading to a “Lotus effect”. The water droplet did not pin to the surface and could roll off the surface at a small tilting angle. This is due to the presence of air pockets between the liquid and surface depressions that was explained by Cassie-Baxter (CB) [22]: $\cos\theta_{CB} = 1 + \varphi_{CB} (\cos\theta_Y + 1)$, where the fraction of solid in contact with the liquid is taken into account with the filling ratio parameter, φ_{CB} (≤1).

3.3 Abrasion due to reciprocating cleaning

The mechanical cleaning of textured PP surfaces was performed in wet and dry conditions and the impact on topographies and CA values were analyzed after 250, 500 and 1000 cycles (see Table 4).

Table 4. Surface topography data and functional response obtained on the textured PP parts after the cleaning cycles.

Number of cleaning cycles (-)	Type of cleaning cycles (-)	True-to-projected area ratio (-)	Peak-to-valley distance (µm)	Water contact angles (°)
0	-	1.728	31.8	159.9
250	wet	1.613	31.1	136.8
500	wet	1.641	27.6	140.3
1000	wet	1.584	23.7	140.8
250	dry	1.445	20.0	132.3
500	dry	1.425	20.3	129.7
1000	dry	1.141	14.3	126.4

The protrusions of the Lotus-inspired topography were the first areas in a tribological contact with the multipurpose cleaning cloth. In dry conditions, the surface was already abraded after 250 cleaning cycles and the topography deteriorated progressively with the increase of the cycles, resulting in CA values of approximately 125° (see Fig. 6-7). In wet conditions, the protrusions were significantly less abraded than those in dry conditions. After 1000 cycles, microtextures with a 1:1 aspect ratio (25 µm Δz over 25 µm spatial distance) and CA of 140° were retained on PP replicas.

3.4. Mould wear after GF-PP moulding cycles

Mould wear was intensified by micromoulding GF reinforced PP parts. Figure 8 depicts the topographies of tool steel surfaces before and after 350 mouldings. The peaks were flattened and free from any laser-induced roughness. Figure 9 shows the flattened valleys on replicas after 25 and 350 GF-PP mouldings.

The true-to-projected aspect ratio and the Δz values decreased progressively with the increase of the moulding cycles (see Table 5 and Fig. 10). In particular, as a result of the mould wear, Δz was reduced to 27 μm after 350 moulding cycles and respectively CA decreased below 150°.

Table 5. Surface topography data and functional response obtained on the textured GF-PP parts after the micromoulding cycles.

Number of injection moulding (-)	True-to-projected area ratio (-)	Peak-to-valley distance (μm)	Water contact angles (°)
0	1.725	31.6	157.4
50	1.712	30.0	-
100	1.716	30.6	-
150	1.711	29.3	-
200	1.686	28.6	-
250	1.688	28.8	-
300	1.695	29.6	-
350	1.684	28.5	143.5

3.5. Discussion

Overall, microtextures with high aspect ratio (≥1) combined with submicron roughness led to superhydrophobicity of PP replicas. Spherical water drops with a higher CA (≥150°) could be observed and the droplets could easily roll-off the surfaces. However, such low wetting was very sensitive to surface damages discussed in Sections 3.3 and 3.4. Especially, any height reduction and damage of micro-textures and partially flattened areas led to an increased spreading of liquid onto the surface and thus lowering the CA values.

Figure 11 summarizes the effects of the two degradation mechanisms observed in this study. The aspect ratios of replicated Lotus-leaf-like topographies decreased as a result of cleaning and moulding cycles. However, wear damage started appearing on the peaks in the case of mechanical cleaning, while the peaks of the replication insert were flattened in the case of abrasive microinjection moulding and this resulted in flattened valleys on GF-PP surfaces.

The decrease of superhydrophobic surface properties can be explained with a transition between CB and W states (see Section 3.2). In particular, the CB state observed on PP replica was metastable and any topographical degradation triggered the imbibition of the surface, i.e. a more stable W state [8]. Lower CAs were observed after the deterioration of micro or submicron textures by either cleaning or moulding cycles. This is in agreement with the W theory, where a lower r_W factor leads to a decrease of CAs.

4. Conclusions

In this research, superhydrophobic polypropylene surfaces were fabricated by micro injection moulding of a laser textured insert. A Lotus-inspired hierarchical topography was replicated on polypropylene parts that incorporate uniform micro-textures with peaks and valleys covered with a laser-induced sub-micron roughness. In spite of the fact that the replication process

was not fully optimized, the textured polymer replicas demonstrated a “Lotus effect”, i.e. high water contact angles were consistently obtained on textured areas.

The effects of surface wear due to reciprocating cleaning (direct abrasion of textured polymer replicas) and abrasive moulding cycles employing glass-fiber reinforced polypropylene (indirect topographical damage due to the mould wear onto the replicas) were investigated. Both abrasive mechanisms had a clear impact on the surface topographies and their respective wetting properties. Direct wear damage on the textured replica resulted in flattened or damaged peaks of the microtextured polypropylene parts. On the contrary, the indirect mould wear damage led to flattened valleys on glass-fiber reinforced polypropylene parts. The superhydrophobic regime was lost as a result of both the cleaning and moulding cycles. The surface damage led to a transition from the Cassie-Baxter to the Wenzel state. In this research, only one surface topography was investigated however it is important to state that the hierarchical topography, i.e. the micro-scale texture, had a beneficial effects. In particular, the replicated Lotus-inspired hierarchical topography allowed the textured surfaces to remain hydrophobic to some extent. Further research should be conducted with other hierarchical topographies that could reinforce the resistant to direct or indirect wear.

Acknowledgments

The research was carried out in the framework of the European Union’s H2020 research and innovation programmes on “Short pulsed laser micro/nanostructuring of surfaces for improved functional applications” (Laser4Fun), “Process fingerprint for zero-defect net-shape micromanufacturing” (MICROMAN), “High-impact injection moulding platform for mass-production of 3D and/or large micro-structured surfaces with antimicrobial, self-cleaning, anti-scratch, anti-squeak and aesthetic functionalities” (HIMALAIA) and “Modular laser based additive manufacturing platform for large scale industrial applications” (MAESTRO). Further support was provided by the UKIERI DST programme “Surface functionalisation for food, packaging, and healthcare applications”.

References

[1] Lapcik, L., Jindrova, P., Lapcikova, B., Tamblyn, R., Greenwood, R., and Rowson N., 2008, “Effect of the talc filler content on the mechanical properties of polypropylene composites,” J. Appl. Polym. Sci., 110(5), pp. 2742 - 2747.

[2] Brezinová, J., and Guzanová, A., 2010, “Friction Conditions during the Wear of Injection Mold Functional Parts in Contact with Polymer Composites,” J. Reinf. Plast. Compos., 29(11), pp. 1712 - 1726.

[3] Zorba, V., Stratakis, E., Barberoglou, M., Spanakis, E., Tzanetakis, P., Anastasiadis, S., and Fotakis, C., 2008, “Biomimetic Artificial Surfaces Quantitatively Reproduce the Water Repellency of a Lotus Leaf,” Adv. Mater., 20(21), pp. 4049 - 4054.

[4] Long, J., Fan, P., Gong, D., Jiang, D., Zhang, H., Li, L., and Zhong, M., 2015, “Superhydrophobic Surfaces Fabricated by Femtosecond Laser with Tunable Water Adhesion: From Lotus Leaf to Rose Petal,” ACS Appl. Mater. Interfaces., 7(18), pp. 9858 - 9865.

[5] Kietzig, A.-M., Hatzikiriakos, S., and Englezos, P., 2009, “Patterned Superhydrophobic Metallic Surfaces,” Langmuir, 25(8), pp. 4821 - 4827.

[6] Baruffi, F., Gulcur, M., Calaon, M., Romano, J.-M., Penchev, P., Dimov, S. S., Whiteside, B. R., and Tosello, G., 2019, “Correlating nano-scale surface replication accuracy and cavity temperature in micro-injection moulding using in-line process control and high-speed thermal imaging,” J. Manuf. Proc., 47, pp. 367 - 381.

[7] Vella, P. C., Dimov, S. S., Brousseau, E., and Whiteside, B. R., 2015, “A new process chain for producing bulk metallic glass replication masters with micro- and nano-scale features,” Int. J. Adv. Manuf. Technol., 76(1-4), pp. 523 - 543.
[8] Romano, J.-M., Gulcur, M., Garcia-Giron, A., Martinez Solanas, E., Whiteside, B. R., and Dimov, S. S., 2019, “Mechanical durability of hydrophobic surfaces fabricated by injection moulding of laser-induced textures,” Appl. Surf. Sci., 476, pp. 850 - 860.
[9] Caffrey, P. O., Nayak, B. K., and Gupta, M. C., 2012, “Ultrafast laser-induced microstructure/nanostructure replication and optical properties,” Appl. Opt., 51(5), pp. 604 - 609.
[10] Nayak, B. K., Caffrey, P. O., Speck, C., and Gupta, M. C., 2013, “Superhydrophobic surfaces by replication of micro/nano-structures fabricated by ultrafast-laser-microtexturing,” Appl. Surf. Sci., 266, pp. 27 - 32.
[11] Falah Toosi, S., Moradi, S., Ebrahimi, M., and Hatzikiriakos, S., 2016, “Microfabrication of polymeric surfaces with extreme wettability using hot embossing,” Appl. Surf. Sci., 378, pp. 426 - 434.
[12] Jiang, D., Fan, P., Gong, D., Long, J., Zhang, H., and Zhong, M., 2016, “High-Temperature Imprinting and Superhydrophobicity of Micro/Nano Surface Structures on Metals Using Molds Fabricated by Ultrafast Laser Ablation,” J. Mater. Process. Technol., 236, pp. 56 - 63.
[13] Rajab, F. H., Liu, Z., Wang, T., and Li, L., 2019, “Controlling Bacteria Retention on Polymer via Replication of Laser Micro/Nano Textured Metal Mould,” Opt. Laser Technol., 111, pp. 530 - 536.
[14] Garcia-Giron, A., Romano, J.-M., Liang, Y., Dashtbozorg, B., Dong, H., Penchev, P., and Dimov, S. S., 2018, “Combined surface hardening and laser patterning approach for functionalising stainless steel surfaces,” Appl. Surf. Sci., 439, pp. 516 - 524.
[15] Garcia-Giron, A., Romano, J.-M., Batal, A., Dashtbozorg, B., Dong, H., Martinez Solanas, E., Urrutia Angos, D., Walker, M., Penchev, P., and Dimov, S. S., 2019, “Durability and wear resistance of laser-textured hardened stainless steel surfaces with hydrophobic properties,” Langmuir, 35(15), pp. 5353 - 5363.
[16] Han, J., Cai, M., Lin, Y., Liu, W., Luo, X., Zhang, H., Wang, K., and Zhong, M., 2018, “Comprehensively durable superhydrophobic metallic hierarchical surfaces via tunable micro-cone design to protect functional nanostructures,” RSC Adv., 8, pp. 6733 - 6744.
[17] Tang, M.-K., Huang, X.-J., Guo, Z., Yu, J.-G., Li, X.-W., and Zhang, Q.-X., 2015, “Fabrication of robust and stable superhydrophobic surface by a convenient, low-cost and efficient laser marking approach,” Colloids Surf. A, 484, pp. 449 - 456.
[18] Su, F., and, Yao, K., 2014, “Facile fabrication of superhydrophobic surface with excellent mechanical abrasion and corrosion resistance on copper substrate by a novel method,” ACS Appl. Mater. Interf., 6, pp. 8762 - 8770.
[19] ASTM D3450-15, 2015, “Standard Test Method for Washability Properties of Interior Architectural Coatings,” ASTM International, West Conshohocken, PA.
[20] Young, T., 1805, “An essay on the cohesion of fluids,” Philos. Trans. R. Soc. Lond., 95, pp. 65 - 87.
[21] Wenzel, R. N., 1936, “Resistance of solid surfaces to wetting by water,” Ind. Eng. Chem., 28(8), pp. 988 - 994.
[22] Cassie, A. B. D., and Baxter, S., 1944, “Wettability of porous surfaces,” Trans. Faraday Soc., 40, pp. 546 - 551.

List of figures:

Fig. 1. Beam line components and the laser scanning strategy.
Fig. 2. Micro injection moulding setup and stages together with the design of the PP replicas.
Fig. 3. Washability tester with multipurpose cloth.
Fig. 4. a-b) Laser-textured mould insert: top view, details and cross-section. c-d) Micromoulded PP: tilted views and top views of representative 1) valley and 2) peak regions.
Fig. 5. Schematic of Young, Wenzel and Cassie-Baxter models.
Fig. 6. The evolution of textured PP surfaces with the increase of cleaning cycles.
Fig. 7. The evolution of topographical metrics and wetting properties with the increase of cleaning cycles.
Fig. 8. The effect of 350 moulding cycles on topography of the insert.
Fig. 9. Flattened valleys of GF-PP replicas after 25 and 350 moulding cycles.
Fig. 10. The evolution of topographical metrics and wetting properties with the increase of moulding cycles.
Fig. 11. A schematic representation of degradation mechanisms and resulting topographies.

Figures

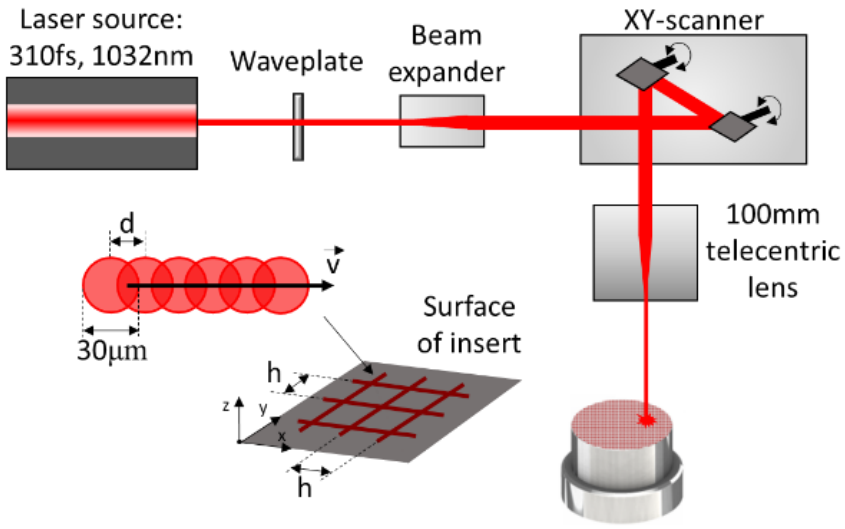

Fig. 1. Beam line components and the laser scanning strategy.

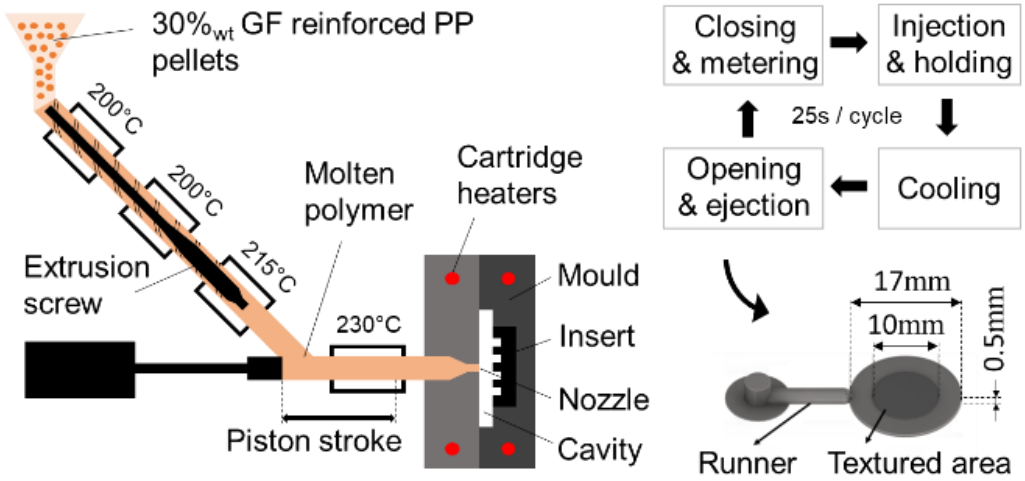

Fig. 2. Micro injection moulding setup and stages together with the design of the PP replicas.

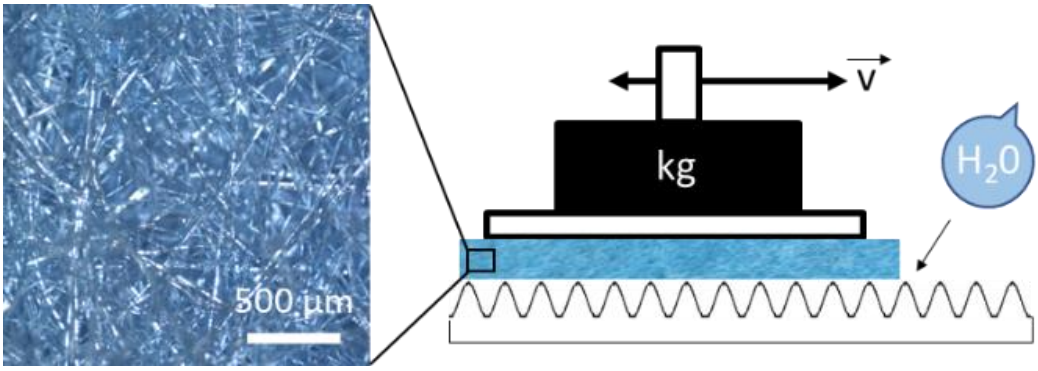

Fig. 3. Washability tester with multipurpose cloth.

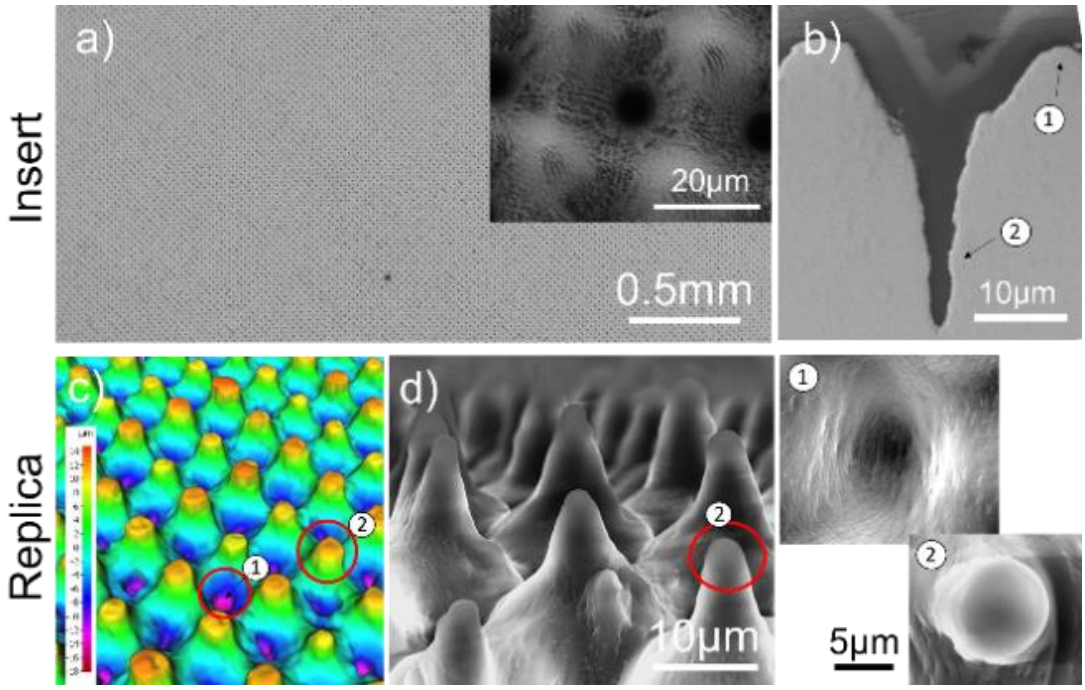

Figure 4. a-b) Laser-textured mould insert: top view, details and cross-section. c-d) Micromoulded PP: tilted views and top views of representative 1) valley and 2) peak regions.

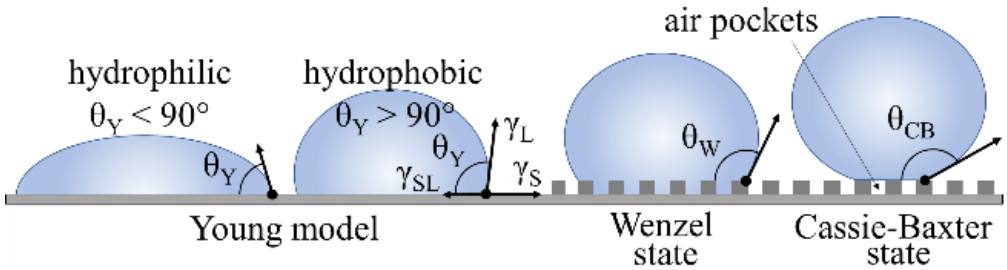

Figure 5. Schematic of Young, Wenzel and Cassie-Baxter models.

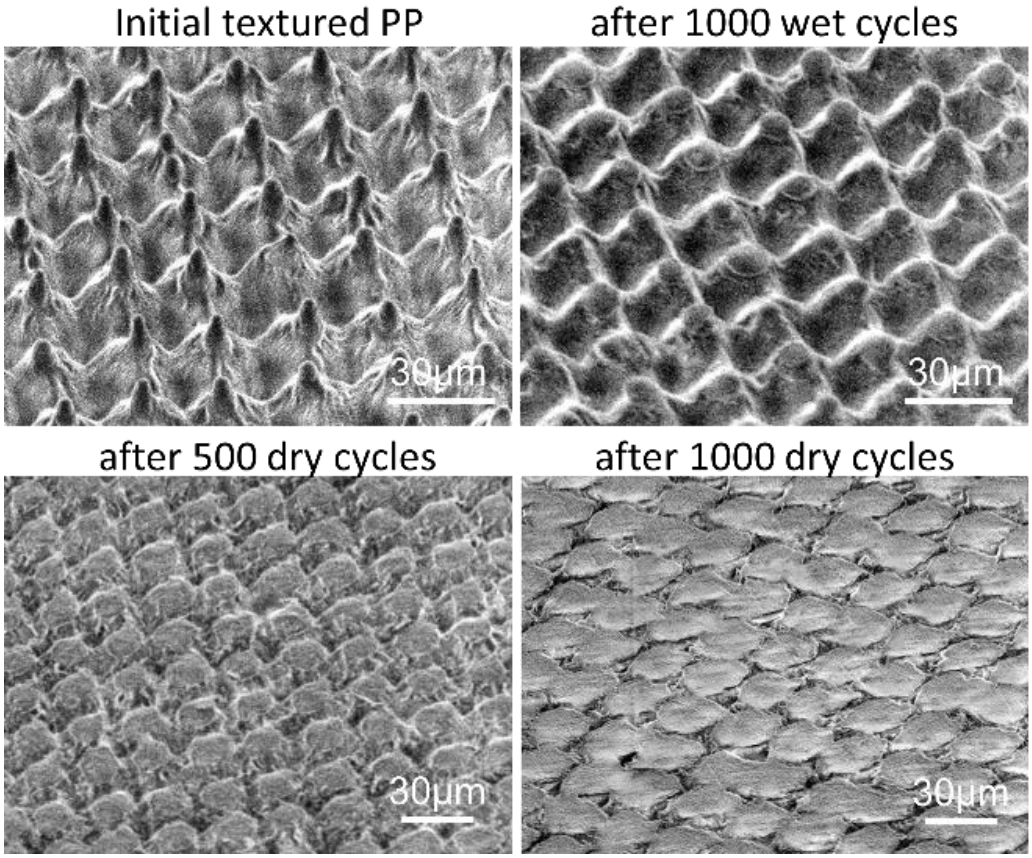

Figure 6. The evolution of textured PP surfaces with the increase of cleaning cycles.

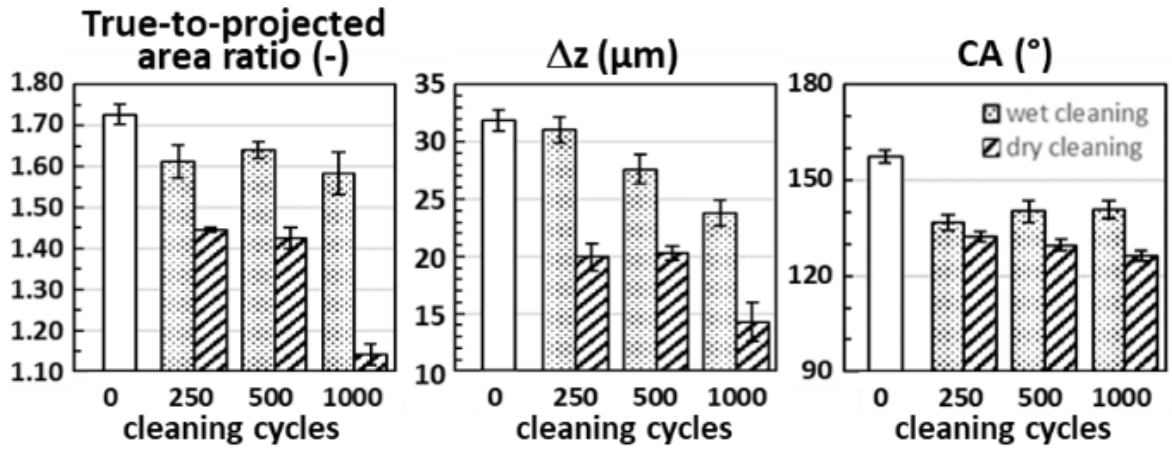

Figure 7. The evolution of topographical metrics and wetting properties with the increase of cleaning cycles.

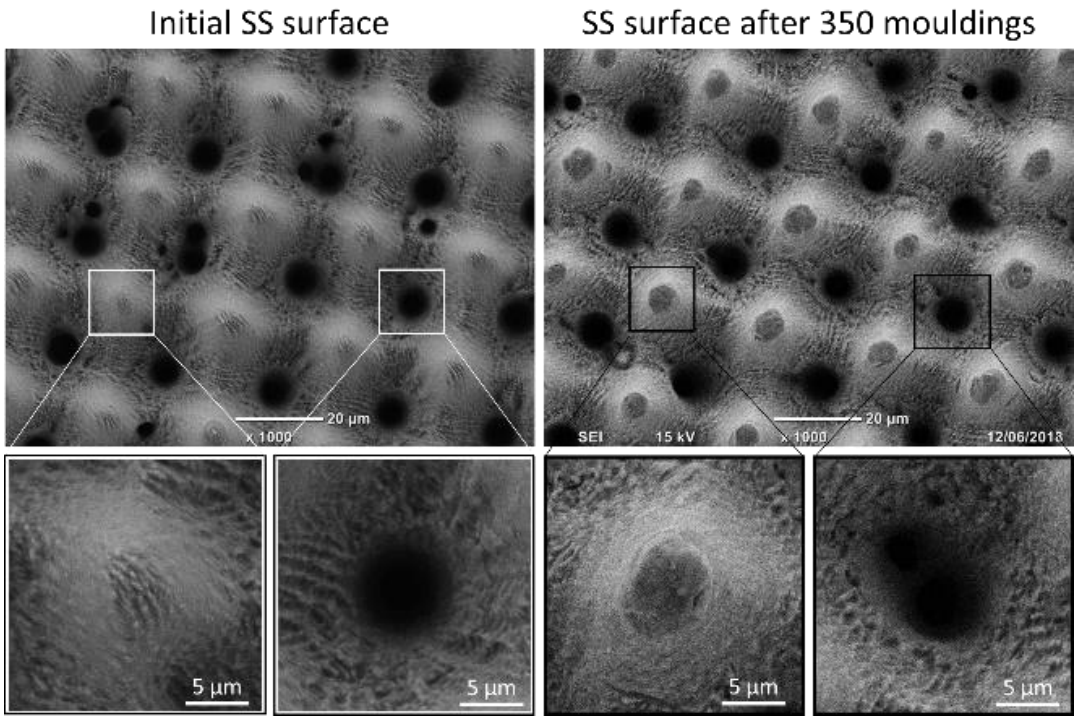

Figure 8. The effect of 350 moulding cycles on topography of the insert.

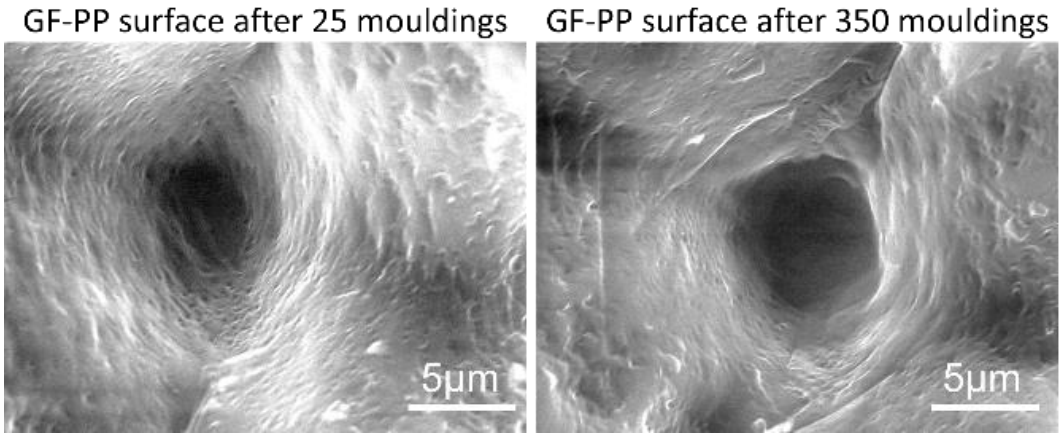

Figure 9. Flattened valleys of GF-PP replicas after 25 and 350 moulding cycles.

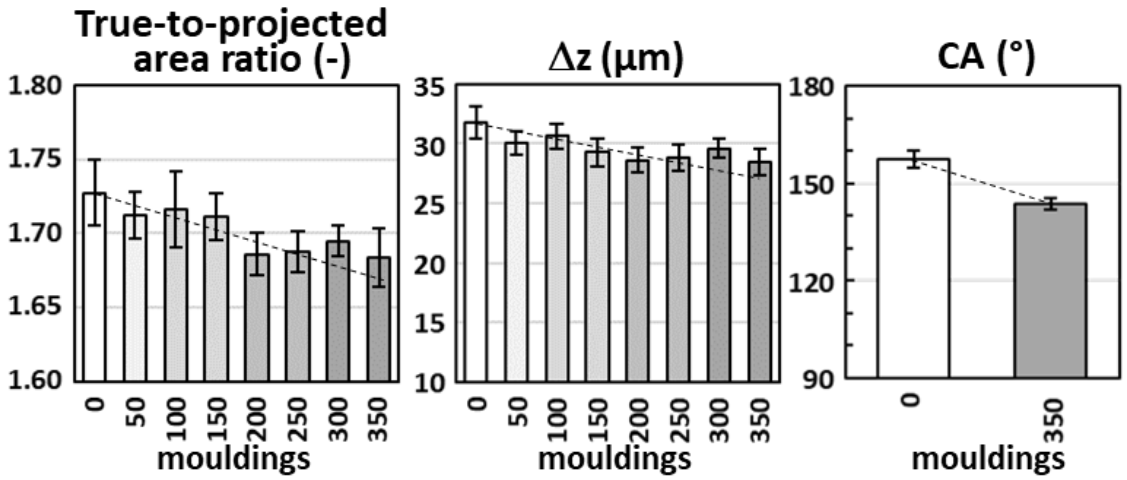

Figure 10. The evolution of topographical metrics and wetting properties with the increase of moulding cycles.

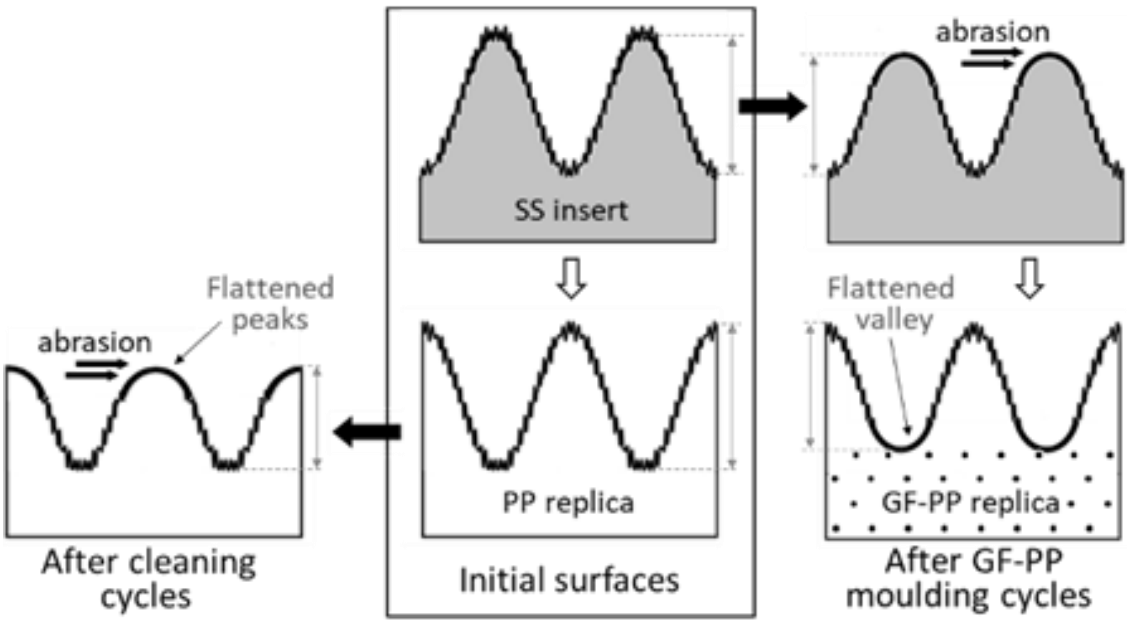

Figure 11. A schematic representation of degradation mechanisms and resulting topographies.